Proc. Estonian Acad. Sci. Chem., 1999, **48**, 2, 80–95
https://doi.org/10.3176/chem.1999.2.02

MODELLING ADVANCED OXIDATION TREATMENT OF POLYCYCLIC AROMATIC HYDROCARBONS

Marjaana HAUTANIEMI[a], Juha KALLAS[a], Rein MUNTER[b], Marina TRAPIDO[b], and Yelena VERESSININA[b]

[a] Department of Chemical Technology, Lappeenranta University of Technology, Box 20, FIN-53851 Lappeenranta, Finland; marjaana.hautaniemi@lut.fi
[b] Department of Environmental Chemistry and Technology, Institute of Chemistry, Tallinn Technical University, Akadeemia tee 15, 12618 Tallinn, Estonia; trapido@chemnet.ee

Received 21 December 1998

Abstract. Oxidation of five polycyclic aromatic hydrocarbons – anthracene, phenanthrene, pyrene, fluoranthene, and benzo(*a*)pyrene – in aqueous solutions with direct photolysis (254 nm), photolysis with hydrogen peroxide, ozonation, ozonation with photolysis, and ozonation combined with hydrogen peroxide and photolysis was studied. A model was developed to describe these processes. An attempt was made to estimate quantum yield from photolysis experiments, reaction rate constant $k_{O3,PAH}$ from ozonolysis experiments, and $k_{OH,PAH}$ from $O_3/H_2O_2/UV$ experiments, and to simulate other advanced oxidation processes using these constants. Under the conditions of the study, the comparison of the simulated and experimental results shows that this kind of approach is feasible even though some difficulties occurred in the evaluation of $k_{OH,PAH}$. Direct ozonation reactions were found to be the dominant pathway of oxidation for all cases studied.

Key words: polycyclic aromatic hydrocarbon, ozone, hydrogen peroxide, UV radiation, advanced oxidation processes, modelling.

INTRODUCTION

Polycyclic aromatic hydrocarbons (PAHs), known as priority pollutants [1], are mainly formed as byproducts of incomplete combustion of fossil fuels. PAHs have been identified in vehicle exhausts, power plant emissions, urban sewage, and emissions from the chemical, coke, and oil-shale industries. Some of them are known to be carcinogenic [2, 3]. The concentration of PAHs in surface waters varies from 0.1 to 830 ng L^{-1} [3]. An EEC Council Directive in 1980 established the maximum contaminant level of 0.2 μg L^{-1} for PAHs in drinking water [4]. The

recommended limit for the total amount of carcinogenic PAHs in drinking water is 0.025 mg L^{-1} [5].

The elimination of PAHs from water is undoubtedly necessary. Although various treatment methods have been applied for this purpose, only oxidation technologies, however, seem to be advisable [6]. Advanced oxidation processes (AOPs) are generally very efficient in oxidizing organic substituents. In AOPs highly reactive hydroxyl radicals are generated using combinations of ozone, hydrogen peroxide, UV radiation, and solid or liquid catalysts. Ozone especially has been found to be a powerful oxidant of PAHs [6, 7]. In addition, oxidation by photolysis seems to have some applicability [6, 7].

Simulation of AOP treatment is complicated due to the large number of chemical species and reactions involved. An ideal model would be capable of describing the processes without empirical parameters that apply only to a particular system. Pedit et al. [8] developed a flexible and extensible model for simulating AOPs. The modelling-based optimization of AOPs has been discussed by Hong et al. [9]. A model is a good tool not only in design or optimization, but also in the estimation of the kinetic parameters of the process. The kinetic constants are typically unknown and their values are extracted from data obtained in laboratory, bench, or pilot scale experiments. In solving a parameter estimation problem the reactor model equations are solved several times during each iterative search of the optimal values of the kinetic parameters. The advantage of this kind of determination is that several parameters can be estimated simultaneously; however, care has to be taken that the parameters do not interfere with each other.

In this study, a model is derived to describe ozone, hydrogen peroxide, and UV radiation involving advanced oxidation of PAHs. An attempt is made to estimate quantum yield from photolysis experiments, reaction rate constant $k_{O3,PAH}$ from ozonation experiments, and $k_{OH,PAH}$ from O_3/H_2O_2/UV experiments, and to simulate other AOPs using these constants. The aim is not to determine exact interpretations of molecular kinetics, but to establish constants applicable for engineering purposes. The modelling is based on the experimental results presented earlier [7].

Photolysis and H_2O_2/UV oxidation

The rate of photoreaction of a chemical C is a function of the rate at which light is absorbed and of the efficiency with which the absorbed light transforms the chemical into the products [10].

$$-\frac{d[C]}{dt} = k_{UV,C} = \phi_C I_0 (1 - \exp(-A_t)) f_C \quad (1)$$

where ϕ_C is the quantum yield of C, that is, the number of molecules undergoing a chemical transformation per photon of light absorbed, and I_0 is

the incident flux of radiation. The factor f_C is the ratio of light absorbed by C to that absorbed by other components of the solution, and A_t is the total absorbance of the solution times a factor 2.3, defined as follows:

$$f_C = \frac{\varepsilon_C [C]}{\Sigma \varepsilon_i [C_i]} \tag{2}$$

$$A_t = 2.3 L \Sigma \varepsilon_i [C_i] \tag{3}$$

where the subscript i represents any species present in the solution that absorbs light at the specified wavelength, L is the effective pathlength of the photoreactor, and ε_i is the molar absorptivity of the ith species at the lamp wavelength.

The photolytic oxidation process can be accelerated by addition of hydrogen peroxide. The photolysis of hydrogen peroxide yields hydroxyl radicals (see reaction 4 in Table 1). Hence, the elimination of organic compounds by H_2O_2/UV treatment has at least two possible routes: direct photolysis (reaction 28) and hydroxyl radical attack (reaction 30). There is, however, a limit for the beneficial effects of added hydrogen peroxide since OH radicals are not only generated by the photolysis of H_2O_2 but are also consumed by H_2O_2 (reactions 11 and 12).

Beltrán et al. [11] studied H_2O_2/UV treatment of fluorene, phenanthrene, and acenaphthene and found that the disappearance rates of PAHs increase substantially with respect to those from UV radiation alone, if suitable hydrogen peroxide concentrations and pH values are established. According to their study, the contribution of direct photolysis to the disappearance of PAHs decreases with increasing hydrogen peroxide concentration and is the main cause of degradation in acidic conditions. Beltrán et al. [12] also determined quantum yields of direct photolysis for PAHs, which were 7.5×10^{-3} for fluorene, 6.9×10^{-3} for phenanthrene, and 52×10^{-3} M^{-1} s^{-1} for acenaphthene.

Ozonation and O_3/H_2O_2 oxidation

At low pH, the ozonation process follows a molecular mechanism. In basic media, however, the process is very complicated due to the formation of different radicals, the most important of which is the hydroxyl radical. These different pathways of reactions lead to different oxidation products, and they are controlled by different kinetics [13]. Ozone is selective in its reactions with organic substances while hydroxyl radical is rather non-selective [14].

Cornell & Kuo [15] studied the reaction between ozone and phenanthrene in aqueous solutions, and found the reaction to be second order, first order with respect to both components. The rate constant increased from 1.94×10^4 M^{-1} s^{-1} in strongly acidic conditions (pH = 2.2) to 4.75×10^4 M^{-1} s^{-1} in neutral conditions at 25 °C.

Butkovic et al. [16] determined the rate constants for the reaction of pyrene, phenanthrene, and benzo(*a*)pyrene with ozone by means of stopped-flow spectrometry. The second-order rate constants determined were 4×10^4, 1.5×10^4, and 0.6×10^4 M^{-1} s^{-1}, respectively, over the pH range of 1–7.

The results by Beltrán et al. [6, 17] on ozonation and O_3/H_2O_2 treatment of PAHs show that because of the importance of the direct reactions the presence of hydrogen peroxide does not improve the oxidation rate compared with ozonation alone. According to their studies [6], ozonation of fluorene is due to both direct and hydroxyl radical reactions, while ozonation of phenanthrene and acenaphthene develops only through direct reactions of ozone. O_3/H_2O_2 oxidation goes through direct and radical reactions in the case of fluorene and phenanthrene, while acenaphthene is removed exclusively by direct ozonation [12]. The molecular ozone reaction rate constants they determined were 2.4×10^3 for phenanthrene, 1.1×10^5 for acenaphthene, and 29 M^{-1} s^{-1} for fluorene at 20°C and pH 7. Beltrán et al. [11] also determined hydroxyl radical rate constants for PAHs, which were 9.9×10^9 for fluorene, 8.8×10^9 for acenaphthene, and 13.4×10^9 M^{-1} s^{-1} for phenanthrene.

O_3/UV and O_3/H_2O_2/UV oxidation

The O_3/UV process is initiated by the photolysis of ozone (see reaction 1 in Table 1). Some investigators suggest that the photolysis of aqueous ozone produces hydroxyl radicals directly, analogously to the gas-phase reaction [18]. Peyton & Glaze [19] propose that the first step is the photolysis of ozone to produce hydrogen peroxide. This step is followed by secondary reactions which produce hydroxyl radicals. The propagation and termination steps are equal to those in the O_3/H_2O_2 system.

Beltrán et al. [12] studied the oxidation of PAHs by ozonation in the presence of UV radiation. According to their study, fluorene was oxidized by direct photolysis, direct ozonation, and hydroxyl radical attack (main pathway) while phenanthrene and acenaphthene were eliminated only through the direct ways, photolysis and ozonation.

EXPERIMENTAL

Ozonation, O_3/H_2O_2, O_3/UV, O_3/H_2O_2/UV, H_2O_2/UV, and photolysis experiments were carried out in a semibatch bubble column, 1.5×10^{-3} m^3 in volume. An ozone–air mixture produced with a laboratory generator was led through the column at a gas flow rate of 1 L min^{-1}. The gas was fed in through a porous glass-plate diffuser 3.0 cm in diameter and with a pore size of 0.16 mm. A low pressure mercury lamp placed in the centre of the column was used as a radiation source. The power output of the lamp at 254 nm was 0.414 W L^{-1}, measured by hydrogen peroxide actinometry [20]. The ozone concentration in the gas phase measured with a spectrophotometer "Specord UV/VIS" at 258 nm, was in the range of 0.1–0.6 mg L^{-1}. Preparation of the

reaction solutions and measuring of PAH concentrations in the ozonized samples have been discussed earlier [7]. The concentrations of PAHs did not exceed their aqueous solubility. Ozonation experiments were conducted at pH 3, 6.5, and 9.5, and the other experiments at pH 6.5.

The experiments with the ozone/hydrogen peroxide system were performed at hydrogen peroxide concentrations from 1×10^{-6} to 2×10^{-5} M.

All experiments were conducted at 20 °C.

KINETIC MODEL

Table 1 presents the mechanism applied to the O_3/UV and O_3/H_2O_2/UV systems. The photolysis reactions of ozone, H_2O_2 and PAH (reactions 1–4 and 28) are excluded in the case of ozonation or O_3/H_2O_2 oxidation. The H_2O_2/UV system consists of reactions 4, 11, 12, 15–18, 22–24, 27, 28, and 30.

Table 1. Reactions and rate constants in O_3/H_2O_2/UV models

No.	Reaction	Rate constant	Reference
1.	$O_3 + h\nu \rightarrow O + O_2$	$k_{UV,O3}$	
2.	$O + H_2O \rightarrow 2\ OH\cdot$	$k_2 = 1.1 \times 10^7\ s^{-1}$	[21]
3.	$O + H_2O \rightarrow H_2O_2$	$k_3 = 2.2 \times 10^8\ s^{-1}$	[21]
4.	$H_2O_2 + h\nu \rightarrow 2\ OH\cdot$	$k_{UV,H2O2}$	
5.	$O_3 + OH^- \rightarrow HO_2\cdot + O_2^{-}\cdot$	$k_5 = 70\ M^{-1}\ s^{-1}$	[22]
6.	$O_3 + HO_2^- \rightarrow HO_2\cdot + O_3^-$	$k_6 = 2.8 \times 10^6\ M^{-1}\ s^{-1}$	[22]
7.	$O_3 + H_2O_2 \rightarrow H_2O + 2O_2$	$k_7 = 0.0065\ M^{-1}\ s^{-1}$	[23]
8.	$O_3 + OH\cdot \rightarrow HO_2\cdot + O_2$	$k_8 = 2 \times 10^9\ M^{-1}\ s^{-1}$	[24]
9.	$O_3 + O_2^{-}\cdot \rightarrow O_3^{-}\cdot + O_2$	$k_9 = 1.6 \times 10^9\ M^{-1}\ s^{-1}$	[24]
10.	$HO_3\cdot \rightarrow OH\cdot + O_2$	$k_{10} = 1.1 \times 10^5\ s^{-1}$	[24]
11.	$OH\cdot + H_2O_2 \rightarrow H_2O + HO_2\cdot$	$k_{11} = 2.7 \times 10^7\ M^{-1}\ s^{-1}$	[25]
12.	$OH\cdot + HO_2^- \rightarrow H_2O + O_2^{-}\cdot$	$k_{12} = 7.5 \times 10^9\ M^{-1}\ s^{-1}$	[25]
13.	$O_3^- + OH\cdot \rightarrow O_2^{-}\cdot + HO_2\cdot$	$k_{13} = 6 \times 10^9\ M^{-1}\ s^{-1}$	[26]
14.	$O_3^- + OH\cdot \rightarrow O_3 + OH^-$	$k_{14} = 2.5 \times 10^9\ M^{-1}\ s^{-1}$	[26]
15.	$HO_2\cdot + O_2^{-}\cdot \rightarrow O_2 + H_2O_2$	$k_{15} = 9.7 \times 10^7\ M^{-1}\ s^{-1}$	[27]
16.	$2OH\cdot \rightarrow H_2O_2$	$k_{16} = 5.5 \times 10^9\ M^{-1}\ s^{-1}$	[25]
17.	$HO_2\cdot + OH\cdot \rightarrow H_2O + O_2$	$k_{17} = 6.6 \times 10^9\ M^{-1}\ s^{-1}$	[25]
18.	$O_2^{-}\cdot + OH\cdot \rightarrow OH^- + O_2$	$k_{18} = 8.0 \times 10^9\ M^{-1}\ s^{-1}$	[25]
19.	$HO_3\cdot + OH\cdot \rightarrow H_2O_2 + O_2$	$k_{19} = 5.0 \times 10^9\ M^{-1}\ s^{-1}$	[21]
20.	$2HO_3\cdot \rightarrow H_2O_2 + 2O_2$	$k_{20} = 5.0 \times 10^9\ M^{-1}\ s^{-1}$	[21]
21.	$HO_3\cdot + O_2^{-}\cdot \rightarrow OH^- + O_2$	$k_{21} = 9.7 \times 10^7\ M^{-1}\ s^{-1}$	[21]
22.	$2HO_2\cdot \rightarrow H_2O_2 + O_2$	$k_{22} = 8.3 \times 10^5\ M^{-1}\ s^{-1}$	[27]
23.	$HO_2\cdot \rightarrow O_2^{-}\cdot + H^+$	$k_{23} = 3.2 \times 10^5\ s^{-1}$	[27]
24.	$O_2^{-}\cdot + H^+ \rightarrow HO_2\cdot$	$k_{24} = 2.0 \times 10^{10}\ M^{-1}\ s^{-}$	[27]
25.	$HO_3\cdot \rightarrow O_3^{-}\cdot + H^+$	$k_{25} = 3.7 \times 10^4\ s^{-1}$	[24]
26.	$O_3^{-}\cdot + H^+ \rightarrow HO_3\cdot$	$k_{26} = 5.2 \times 10^{10}\ M^{-1}\ s^{-1}$	[24]
27.	$H_2O_2 \leftrightarrow H^+ + HO_2^-$	$pK_{28} = 11.6$	[14]
28.	PAH + hν → Products	$k_{UV,PAH}$	
29.	O_3 + PAH → Products	$k_{O3,PAH}$	
30.	OH· + PAH → Products	$k_{OH,PAH}$	

Assuming that the kinetic regime is slow and the chemical reactions take place only in the liquid phase, the rates of depletion and formation of the different species in a completely mixed isothermal semicontinuous column can be formulated as follows:

$$\frac{d[O_3(l)]}{dt} = k_L a\left(\frac{[O_3(g)]}{He} - [O_3(l)]\right) - k_{UV,O3} - k_5[O_3(l)][OH^-] - k_6[O_3(l)][HO_2^-]$$
$$- k_7[O_3(l)][H_2O_2] - k_8[O_3(l)][OH\cdot] - k_9[O_3(l)][O_2^-\cdot]$$
$$+ k_{14}[O_3^-\cdot][OH\cdot] - k_{03,PAH}[O_3(l)][PAH] \tag{4}$$

where $[O_3(l)]$ refers to ozone concentration in the bulk of the liquid phase and $[O_3(g)]$ to ozone concentration in the gas stream leaving the liquid phase. *He* is the Henry's law constant of ozone and $k_L a$ the ozone mass transfer coefficient in the liquid.

$$\frac{d[PAH]}{dt} = -k_{UV,PAH} - k_{O3,PAH}[O_3(l)][PAH] - k_{OH,PAH}[OH\cdot][PAH] \tag{5}$$

$$\frac{d[H_2O_2]_{tot}}{dt} = k_3[O] - k_{UV,H2O2} - k_6[O_3(l)][HO_2^-] - k_7[O_3(l)][H_2O_2]$$
$$- k_{11}[OH\cdot][H_2O_2] - k_{12}[OH\cdot][HO_2^-] + k_{15}[HO_2\cdot][O_2^-\cdot] \tag{6}$$
$$+ k_{16}[OH\cdot]^2 + k_{19}[OH\cdot][HO_3\cdot] + k_{20}[HO_3\cdot]^2 + k_{22}[HO_2\cdot]^2$$

$$[H_2O_2]_{tot} = [H_2O_2] + [HO_2^-] \tag{7}$$

$$\frac{d[OH\cdot]}{dt} = 2k_2[O] - 2k_{UV,H2O2} - k_8[O_3(l)][OH\cdot] + k_{10}[HO_3\cdot]$$
$$- k_{11}[OH\cdot][H_2O_2] - k_{12}[OH\cdot][HO_2^-] - k_{13}[O_3^-\cdot][OH\cdot]$$
$$- k_{14}[O_3^-\cdot][OH\cdot] - 2k_{16}[OH\cdot]^2 - k_{17}[HO_2\cdot][OH\cdot] \tag{8}$$
$$- k_{18}[O_2^-\cdot][OH\cdot] - k_{19}[OH\cdot][HO_3\cdot] - k_{OH,PAH}[OH\cdot][PAH]$$

$$\frac{d[O]}{dt} = k_{O3,UV} - k_2[O] - k_3[O] \tag{9}$$

$$\frac{d[O_2^- \cdot]}{dt} = k_5[O_3(l)][OH^-] - k_9[O_3(l)][O_2^- \cdot] + k_{12}[OH \cdot][HO_2^-] + k_{13}[O_3^- \cdot][OH \cdot] - k_{15}[HO_2 \cdot][O_2^- \cdot] - k_{18}[O_2^- \cdot][OH \cdot] - k_{21}[HO_3 \cdot][O_2^- \cdot] + k_{23}[HO_2 \cdot] - k_{24}[O_2^- \cdot][H^+] \quad (10)$$

$$\frac{d[HO_2 \cdot]}{dt} = k_5[O_3(l)][OH^-] + k_6[O_3(l)][HO_2^-] + k_8[O_3(l)][OH \cdot] + k_{11}[OH \cdot][H_2O_2] + k_{13}[O_3^- \cdot][OH \cdot] - k_{15}[HO_2 \cdot][O_2^- \cdot] - k_{17}[HO_2 \cdot][OH \cdot] - 2k_{22}[HO_2 \cdot]^2 - k_{23}[HO_2 \cdot] + k_{24}[O_2^- \cdot][H^+] \quad (11)$$

$$\frac{d[O_3^- \cdot]}{dt} = k_6[O_3(l)][HO_2^-] + k_9[O_3(l)][O_2^- \cdot] - k_{13}[O_3^- \cdot][OH \cdot] - k_{14}[O_3^- \cdot][OH \cdot] + k_{25}[HO_3 \cdot] - k_{26}[O_3^- \cdot][H^+] \quad (12)$$

$$\frac{d[HO_3 \cdot]}{dt} = -k_{10}[HO_3 \cdot] - k_{19}[OH \cdot][HO_3 \cdot] - 2k_{20}[HO_3 \cdot]^2 - k_{21}[HO_3 \cdot][O_2^- \cdot] - k_{25}[HO_3 \cdot] + k_{26}[O_3^- \cdot][H^+] \quad (13)$$

$$V_G \frac{d[O_3(g)]}{dt} = Q_G\left([O_3(g)]_{in} - [O_3(g)]\right) - k_L a\left(\frac{[O_3(g)]}{He} - [O_3(l)]\right)V_L \quad (14)$$

where Q_G is the gas volumetric flow rate, V_L liquid volume in the reactor, V_G gas content in the reactor, and $[O_3(g)]_{in}$ the ozone concentration in the gas feed. To determine the gas content in the porous glass-plate diffusor, the gas hold-up $(=V_G/(V_G+V_L))$ was calculated based on the correlation presented by Sotelo et al. [28].

In the derivation of the model, it was assumed that the highly reactive radicals come rapidly to a stationary state concentration, which can be calculated by setting the production rate of the radicals equal to the rate at which they are destroyed. The steady state approximations were used for OH, O_2^-, HO_2, O_3^-, and HO_3 radicals, and for the oxygen atom O. The polycyclic organic compounds under study have high molecular weights and their volatilization was neglected.

The photolysis decomposition rates of PAHs, ozone, and hydrogen peroxide were calculated according to Eqs. (1)–(3). The extinction coefficients (in

$M^{-1}\,cm^{-1}$) determined experimentally at 254 nm were 61 600 for anthracene, 23 000 for phenanthrene, and 29 500 for pyrene. For fluoranthene and benzo(*a*)pyrene the values measured in ethanol [3], respectively 14 790 and 45 700 $M^{-1}\,cm^{-1}$, were used. The molar extinction coefficient for ozone at 254 nm is 3300 $M^{-1}\,cm^{-1}$ [29] and for hydrogen peroxide 19.6 $M^{-1}\,cm^{-1}$ [30]. The quantum yields for ozone and hydrogen peroxide were taken as 0.62 mol $einstein^{-1}$ [31] and 0.5 mol $einstein^{-1}$ [30].

The ozone volumetric mass transfer coefficient determined experimentally was relatively high, 0.023 s^{-1}, due to the very intensive mixing in a small contactor. The gas–liquid partition coefficient for ozone at 20 °C was taken as 3.30 [32]. The incident flux of radiation in the reactor was 8.8×10^{-7} einstein $L^{-1}\,s^{-1}$ and the effective path length of radiation was 3.3 cm. A value of 4×10^{-4} m s^{-1}, obtained by applying the Calderbank equation [33], was used for k_L in order to calculate the Hatta numbers. The molecular diffusion coefficient of ozone was taken as 1.26×10^{-9} $m^2\,s^{-1}$ [34].

The equations obtained were solved numerically using Livermore Solver for Ordinary Differential Equations (LSODE) with automatic switching method for stiff and nonstiff problems [35, 36]. A nonlinear constrained global optimization method with random search and simplex booster developed by Palosaari et al. [37] was applied in the parameter estimation. The objective function used in the estimations was

$$F_{obj} = w\sum\left([PAH]_{Exp.} - [PAH]_{Calc.}\right)^2 \qquad (15)$$

where w is a scale constant. The numerical values of $[PAH]_{Calc.}$ needed in the parameter estimation have to be computed during the estimation, which implies that the reactor model described above exists as a subroutine for the parameter estimation routine.

RESULTS AND DISCUSSION

The aim of the study was to estimate $k_{O3,PAH}$ from ozonolysis experiments, quantum yield from photolysis experiments, and $k_{OH,PAH}$ from O_3/H_2O_2/UV experiments, and to be able to simulate other AOPs using these constants. When estimating the rate constants for the reaction between ozone and PAH, it was assumed that pH in the experiments was low enough for hydroxyl radical reactions to be neglected. Table 2 presents the reaction rate constants obtained. Comparison with the values found in the literature shows that the value calculated for phenanthrene agrees with the values measured by Cornell & Kuo [15]; however, the value determined for phenanthrene by Beltrán et al. [6] is considerably lower. The values determined for phenanthrene and pyrene agree

with the values obtained by Butkovic et al. [16], but the value obtained for benzo(*a*)pyrene is considerably higher. The rate constants shown in Table 2 are somewhat higher than those reported previously on the basis of the same experiments [7]. No data on the liquid phase ozone concentrations were available, which brings some inaccuracy into the results of both approaches. In the previous study, when determining the rate constants, the liquid phase ozone concentrations were calculated from the ozone concentrations in the outlet gas utilizing the ozone solubility coefficient in water. However, data from the very beginning of the reaction were lacking. The model used in the estimation in this study requires additional information such as mass transfer coefficients, which may have some influence on the results. As to the inaccuracies of both methods, the results are within acceptable limits. The concentrations of ozone in the outlet gas were not used in the estimation, however, the simulated values were found to correspond to the experimental values. When deriving the model, it was assumed that PAH decomposition proceeds in the regime of slow chemical reactions. The Hatta numbers calculated for the reaction between ozone and PAH are <0.3, indicating that the reactions are slow (see Table 2).

Table 2. Rate constants and Hatta numbers (*Ha*) calculated for the reaction between ozone and PAH

Compound	$k_{O3,PAH}$, $M^{-1}\ s^{-1}$	$Ha = (k_{O3,PAH} D_{O3}[PAH])^{1/2}/k_L$
Anthracene (pH = 6.5)	6.6×10^4	0.014
Phenanthrene (pH = 3.0)	2.7×10^4	0.033
Pyrene (pH = 6.5)	7.7×10^4	0.011
Fluoranthene (pH = 3.0)	6.1×10^3	0.007
Benzo(*a*)pyrene (pH = 3.0)	3.4×10^5	0.003

D, molecular diffusion coefficient, $m^2\ s^{-1}$.

The quantum yields (in mol einstein^{-1}) determined from the photolysis experiments at 254 nm based on the Eqs. (1)–(3) were 0.0075 for anthracene, 0.0020 for phenanthrene, 0.050 for pyrene, 0.028 for fluoranthene, and 0.043 for benzo(*a*)pyrene. Comparison with the values found in the literature for similar compounds shows that they are in the same order of magnitude [12, 38].

Table 3 shows the k_{OH} values estimated from the $O_3/H_2O_2/UV$ experiment. The fact that they are at least one order of magnitude lower than those determined for similar compounds, such as $5 \times 10^9\ M^{-1}\ s^{-1}$ and $1.2 \times 10^{10}\ M^{-1}\ s^{-1}$ determined for naphthalene [25], could be due to the unimportance of the hydroxyl radical reactions under the conditions used in this study. It is also possible that some hydroxyl radicals consuming intermediates are formed. Neglecting their existence leaves more hydroxyl radicals for PAH decomposition and thus might make the rate constants smaller.

Table 3. Hydroxyl radical reaction rate constants calculated from O_3/H_2O_2/UV experiments

Compound	$k_{OH,PAH}$, $M^{-1}\ s^{-1}$
Anthracene	2.5×10^7
Phenanthrene	1.1×10^7
Pyrene	1.7×10^6
Fluoranthene	8.5×10^6
Benzo(*a*)pyrene	3.2×10^8

Despite the low $k_{OH,PAH}$ values obtained, the O_3 (pH = 9.5), O_3/H_2O_2, O_3/UV, and H_2O_2/UV oxidations of PAHs were simulated using the constants estimated. Figures 1–6 display the results obtained.

In the case of anthracene and pyrene, the simulations agreed well with the experimental data, examples of which can be seen in Figs. 1 and 2. For fluoranthene, all the simulations predicted slower decomposition than was observed in the experiments, an example of which is seen in Fig. 3. For benzo(*a*)pyrene, the decomposition observed in the experiments at the beginning of the oxidation was faster than predicted by the simulations (Fig. 4). In the case of phenanthrene, some variation in the success of the simulations can be observed (Figs. 5 and 6). In the simulation of O_3/H_2O_2 and O_3/UV oxidation, the decomposition predicted by the model was slightly slower than observed in the experiments. However, in the case of H_2O_2/UV treatment and ozonation at pH 9.5, the simulations predicted faster decomposition than obtained in the experiments.

Even though the constants obtained in this study are restricted to limited conditions, the comparisons above demonstrate that prediction of the behaviour of one AOP using the data of another AOP is possible. Naturally, if the composition of the water matrix varies, for example, several other species are present, the models have to include these variations. To get a 'real' $k_{OH,PAH}$ with this approach, complementary detailed experimental data, for example, on the formation of all the products, would be needed so that a detailed model could be built.

The importance of molecular ozonation in the decomposition of PAHs by advanced oxidation treatment in the conditions of this study can be illustrated by comparing the magnitude of the terms of Eq. (5) at the half-life time. According to the simulations, both ozonation in acidic conditions and O_3/H_2O_2 treatment of all the compounds under study are due to molecular ozonation. These findings are in good agreement with the results of Beltrán et al. [6]. Simulation of ozonation at higher pH values shows that the role of the hydroxyl radical attack increases as a function of pH, however, the half-life time seems to increase rapidly as well.

Similar comparisons of the other AOPs at the half-life time show that both O_3/UV and O_3/H_2O_2/UV treatments of phenanthrene proceed mainly through

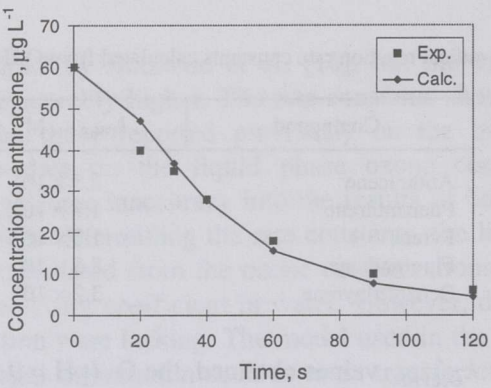

Fig. 1. O_3/H_2O_2 oxidation of anthracene. Experimental vs. simulated concentrations. Conditions: $[Anthracene]_0 = 60\ \mu g\ L^{-1}$, $[O_3]_0 = 0.216\ mg\ L^{-1}$, $[H_2O_2]_0 = 0.068\ mg\ L^{-1}$, pH = 6.5.

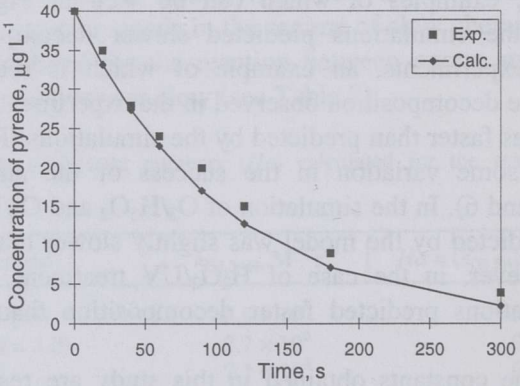

Fig. 2. H_2O_2/UV oxidation of pyrene. Experimental vs. simulated concentrations. Conditions: $[Pyrene]_0 = 40\ \mu g\ L^{-1}$, $[H_2O_2]_0 = 16.5\ mg\ L^{-1}$, $I_0 = 8.77 \times 10^{-7}$ einstein $L^{-1}\ s^{-1}$, pH = 6.5.

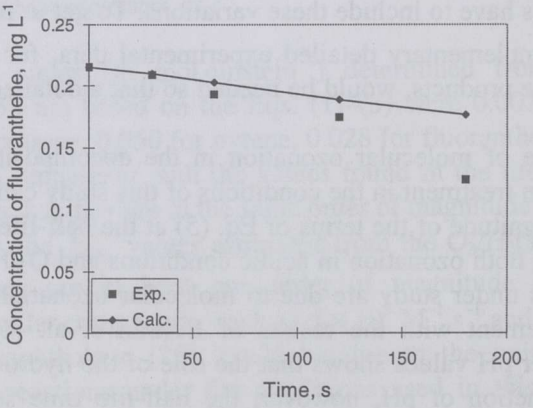

Fig. 3. Ozonation of fluoranthene. Experimental vs. simulated concentrations. Conditions: $[Fluoranthene]_0 = 0.215\ mg\ L^{-1}$, $[O_3]_0 = 0.240\ mg\ L^{-1}$, pH = 9.5.

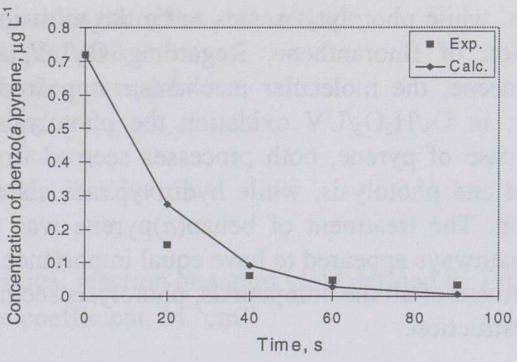

Fig. 4. O_3/UV oxidation of benzo(*a*)pyrene. Experimental vs. simulated concentrations. Conditions: $[\text{Benzo}(a)\text{pyrene}]_0 = 0.718\ \mu g\ L^{-1}$, $[O_3]_0 = 0.165\ mg\ L^{-1}$, $I_0 = 8.77 \times 10^{-7}$ einstein $L^{-1}\ s^{-1}$, pH = 6.5.

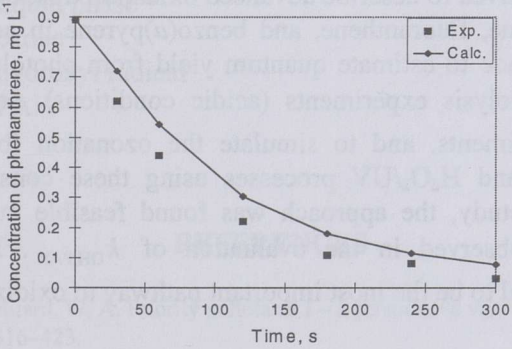

Fig. 5. O_3/UV oxidation of phenanthrene. Experimental vs. simulated concentrations. Conditions: $[\text{Phenanthrene}]_0 = 0.89\ mg\ L^{-1}$, $[O_3]_0 = 0.47\ mg\ L^{-1}$, $I_0 = 8.77 \times 10^{-7}$ einstein $L^{-1}\ s^{-1}$, pH = 6.5.

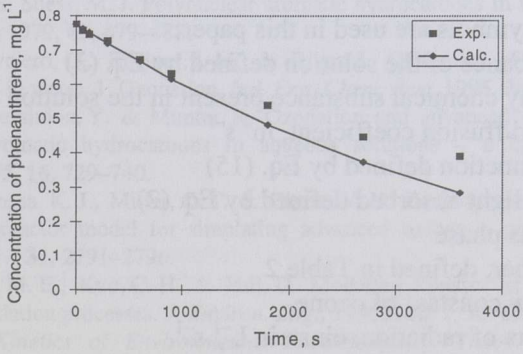

Fig. 6. H_2O_2/UV oxidation of phenanthrene. Experimental vs. simulated concentrations. Conditions: $[\text{Phenanthrene}]_0 = 0.89\ mg\ L^{-1}$, $[H_2O_2]_0 = 16.5\ mg\ L^{-1}$, $I_0 = 8.77 \times 10^{-7}$ einstein $L^{-1}\ s^{-1}$, pH = 6.5.

molecular ozonation, while photolysis seems to be the most important pathway in the decomposition of fluoranthene. Regarding O_3/UV and O_3/H_2O_2/UV treatments of anthracene, the molecular mechanism appeared to be the most important; however, in O_3/H_2O_2/UV oxidation the photolysis also had some importance. In the case of pyrene, both processes seemed to proceed through molecular ozonation and photolysis, while hydroxyl radicals did not have any role in the oxidation. The treatment of benzo(*a*)pyrene was the only process where all the three pathways appeared to have equal importance.

In H_2O_2/UV treatment of all the compounds, photolysis seemed to be the most important way of destruction.

SUMMARY

A model was derived to describe advanced oxidation treatment of anthracene, phenanthrene, pyrene, fluoranthene, and benzo(*a*)pyrene in aqueous solutions. An attempt was made to estimate quantum yield from photolysis experiments, $k_{O3,PAH}$ from ozonolysis experiments (acidic conditions), and $k_{OH,PAH}$ from O_3/H_2O_2/UV experiments, and to simulate the ozonation (basic conditions), O_3/UV, O_3/H_2O_2, and H_2O_2/UV processes using these constants. Under the conditions of the study, the approach was found feasible even though some difficulties were observed in the evaluation of $k_{OH,PAH}$. Direct ozonation reactions were found to be the most important pathway to oxidize PAHs.

APPENDIX

NOTATION

The following symbols are used in this paper:

A_t	total absorbance of the solution defined by Eq. (3)
C	refers to any chemical substance present in the solution in Eq. (1)–(3)
D	molecular diffusion coefficient, $m^2\ s^{-1}$
F_{obj}	objective function defined by Eq. (15)
f	fraction of light absorbed defined by Eq. (2)
g	refers to gas phase
Ha	Hatta number, defined in Table 2
He	Henry's law constant of ozone
I_0	incident flux of radiation, einstein $L^{-1}\ s^{-1}$
k	reaction rate constant, $M^{-1}\ s^{-1}$ or s^{-1}
k_{UV}	photolysis rate constant defined by Eq. (1), $M^{-1}\ s^{-1}$
k_La	liquid phase volumetric mass transfer coefficient, s^{-1}
k_L	liquid phase mass transfer coefficient, $m\ s^{-1}$

L effective pathlength of the photoreactor, cm
l refers to liquid phase
Q volumetric flow rate, $m^3\ s^{-1}$
$t_{½}$ half-life time, s
V volume, m^3
w scale constant in Eq. (15)

Greek letters

ϕ photochemical reaction quantum yield defined by Eq. (1), mol $einstein^{-1}$
ε extinction coefficient, $M^{-1}cm^{-1}$

Subscripts

G refers to gas phase
H2O2 refers to hydrogen peroxide
in refers to gas feed
L refers to liquid phase
O3 refers to ozone
OH refers to hydroxyl radical
PAH refers to PAH
tot total

REFERENCES

1. Keith, L. H. & Telliard, W. A. Priority pollutants I – a perspective view. *Environ. Sci. Technol.*, 1979, **13**, 4, 416–423.
2. Menzie, C. A., Potocki, B. B. & Santodonato, J. Exposure to the carcinogenic PAHs in the environment. *Environ. Sci. Technol.*, 1992, **26**, 1278–1284.
3. Clar, E. *Polycyclic Hydrocarbons*, Vol. 1. Academic Press, London, 1964.
4. Sayre, I. M. International standards for drinking water. *J. Am. Water Works Assoc.*, 1988, **80**, 53–60.
5. Andelman, J. B. & Suess, M. J. Polynuclear aromatic hydrocarbons in the water environment. *Bull. W.H.O.*, 1979, **43**, 479–488.
6. Beltrán, F. J., Ovejero, G., Encinar, J. M. & Rivas, J. Oxidation of polynuclear aromatic hydrocarbons in water. 1. Ozonation. *Ind. Eng. Chem. Res.*, 1995, **34**, 5, 1596–1606.
7. Trapido, M., Veressinina, Y. & Munter, R. Ozonation and advanced oxidation processes of polycyclic aromatic hydrocarbons in aqueous solutions – a kinetic study. *Environ. Technol.*, 1995, **16**, 729–740.
8. Pedit, J. A., Iwamasa, K. J., Miller, C. T. & Glaze, W. H. Development and application of a gas-liquid contactor model for simulating advanced oxidation processes. *Environ. Sci. Technol.*, 1997, **31**, 2791–2796.
9. Hong, A., Zappi, M. E., Kuo, C. H. & Hill, D. Modeling kinetics of illuminated and dark advanced oxidation processes. *J. Environ. Eng.*, 1996, **122**, 1, 58–62.
10. Leifer, A. *The Kinetics of Environmental Photochemistry. Theory and Practice.* ACS Professional Reference Book, York, PA, 1988.
11. Beltrán, F. J., Ovejero, G. & Rivas, J. Oxidation of polynuclear aromatic hydrocarbons in water. 3. UV radiation combined with hydrogen peroxide. *Ind. Eng. Chem. Res.*, 1996, **35**, 3, 883–890.

12. Beltrán, F. J., Ovejero, G., Garcia-Araya, J. F. & Rivas, J. Oxidation of polynuclear aromatic hydrocarbons in water. 2. UV radiation and ozonation in the presence of UV radiation. *Ind. Eng. Chem. Res.*, 1995, **34**, 5, 1607–1615.
13. Staehelin, J. & Hoigné, J. Decomposition of ozone in water in the presence of organic solutes acting as promoters and inhibitors of radical reactions. *Environ. Sci. Technol.*, 1985, **19**, 12, 1206–1213.
14. Langlais, B., Reckhow, D. A. & Brink, D. R. *Ozone in Water Treatment – Application and Engineering*. Lewis Publishers, Chelsea, Michigan, 1991.
15. Cornell, L. P. & Kuo, C. H. A kinetic study of ozonation of phenanthrene in aqueous solutions. *Trans. Air Pollut. Control Assoc.*, 1984, March, 275–286.
16. Butkovic, V., Klasinc, L., Orhanovic, M., Turk, J. & Güsten, H. Reaction rates of polynuclear aromatic hydrocarbons with ozone in water. *Environ. Sci. Technol.*, 1983, **17**, 8, 546–548.
17. Beltrán, F. J., Ovejero, G. & Rivas, J. Oxidation of polynuclear aromatic hydrocarbons in water. 4. Ozone combined with hydrogen peroxide. *Ind. Eng. Chem. Res.*, 1996, **35**, 3, 891–898.
18. Okabe, H. *Photochemistry of Small Molecules*. Wiley-Interscience, New York, 1978.
19. Peyton, G. R. & Glaze, W. H. Destruction of pollutants in water with ozone in combination with ultraviolet radiation. 3. Photolysis of aqueous ozone. *Environ. Sci. Technol.*, 1988, **22**, 7, 761–767.
20. Nicole, I., De Laat, J., Doré, M., Duguet, J.-P. & Bonnel, C. Utilisation du rayonnement ultraviolet dans le traitement des eaux: measure du flux photonique par actinométrie chimique au peroxyde d'hydrogène. *Water Res.*, 1990, **24**, 157–168.
21. Yao, C. C. D., Haag, W. R. & Mill, T. Kinetic features of advanced oxidation processes for treating aqueous chemical mixtures. In *Proc. 2nd Int. Symp. on Chemical Oxidation: Technologies for the Nineties, Nashville, Tennessee, February 19–21, 1992*, Vol. 2, 112–139.
22. Staehelin, J. & Hoigné, J. Decomposition of ozone in water: Rate of imitiation by hydroxide ions and hydrogen peroxide. *Environ. Sci. Technol.*, 1982, **16**, 10, 676–681.
23. Neta, P., Huie, R. E. & Ross, A. B. Rate constants for reactions of inorganic radicals in aqueous solution. *J. Phys. Chem. Ref. Data*, 1988, **17**, 3, 1027–1284.
24. Bühler, R. E., Staehelin, J. & Hoigné, J. Ozone decomposition in water studied by pulse radiolysis. 1. HO_2/O_2^- and HO_3/O_3^- as intermediates. *J. Phys. Chem.*, 1984, **88**, 12, 2560–2564.
25. Buxton, G. V., Greenstock, C. L., Helman, W. P. & Ross, A. B. Critical review of rate constants for reactions of hydrated electrons, hydrogen atoms and hydroxyl radical ($\cdot OH/\cdot O^-$) in aqueous solution. *J. Phys. Chem. Ref. Data*, 1988, **17**, 2, 513–886.
26. Tomiyasu, H., Fukutomi, H. & Gordon, G. Kinetics and mechanism of ozone decomposition in basic aqueous solution. *Inorg. Chem.*, 1985, **24**, 19, 2962–2966.
27. Bielski, B. H. J., Cabelli, D. E., Arudi, R. L. & Ross, A. B. Reactivity of HO_2/O_2^- radicals in aqueous solution. *J. Phys. Chem. Ref. Data*, 1985, **14**, 4, 1041–1100.
28. Sotelo, J. L., Benitez, F. J., Beltran-Heredia, J. & Rodriguez, C. Gas holdup and mass transfer coefficients in bubble columns. 1. Porous glass-plate diffusers. *Int. Chem. Eng.*, 1994, **34**, 1, 82–90.
29. Gordon, G., Pacey, G. E., Cooper, W. J. & Rice, R. G. The chemical reactions of ozone and their role in developing improved analytical methods. *Ozone Sci. Eng.*, 1988, **10**, 89–102.
30. Baxendale, J. H. & Wilson, J. A. Photolysis of hydrogen peroxide at high light intensities. *Trans. Faraday Soc.*, 1957, **53**, 344–356.
31. Taube, H. Photochemical reactions of ozone in solution. *Trans. Faraday Soc.*, 1957, **53**, 656–665.
32. Kosak-Channing, L. F. & Helz, G. R. Solubility of ozone in aqueous solutions of 0–0.6 M ionic strength at 5–30 °C. *Environ. Sci. Technol.*, 1983, **17**, 3, 145–149.
33. Froment, G. F. & Bischoff, K. B. *Chemical Reactor Analysis and Design*. John Wiley and Sons, New York, 1979.

34. Matrozov, V., Kashtanov, S. & Stepanov, A. Experimental determination of the molecular diffusion coefficient of ozone in water. *Zh. Prikl. Khim.*, 1976, **49**, 1070–1073 (in Russian).
35. Hindmarsh, A. ODEPACK, a systematized collection of ODE solvers, Lawrence Livermore Laboratory. In *Scientific Computing* (Stepleman, R. S. et al., eds.). IMACS North Holland Publishing Company, Amsterdam, 1983, 55–64.
36. Petzold, L. R. Automatic selection of methods for solving stiff and nonstiff systems of ordinary differential equations. *Siam. J. Sci. Stat. Comput.*, 1983, **4**, 136–148.
37. Palosaari, S., Parviainen, S., Hiironen, J., Reunanen, J. & Neittaanmäki, P. A random search optimizer algorithm for constrained global optimization. *Acta Polytech. Scand., Chem. Technol Metall. Ser.*, 1986, 172.
38. Tuhkanen, T. *Oxidation of Organic Compounds in Water and Waste Water with the Combination of Hydrogen Peroxide and UV Radiation.* PhD Dissertation, University of Kuopio, Finland, 1994.

POLÜAROMAATSETE SÜSIVESINIKE TÄIUSTATUD OKSÜDATSIOONIPROTSESSIDE MODELLEERIMINE

Marjaana HAUTANIEMI, Juha KALLAS, Rein MUNTER, Marina TRAPIDO ja Jelena VERESSININA

Uuriti viie polüaromaatse süsivesiniku antratseeni, fenantreeni, püreeni, fluoranteeni ja benso(*a*)püreeni oksüdatsiooni vesilahuses kasutades UV-kiirgust (254 nm), UV/H_2O_2, osooni (O_3), O_3/UV ja O_3/H_2O_2/UV. Töötati välja neid protsesse kirjeldavad matemaatilised mudelid. Fotolüüsi katseandmetest määrati kvantsaagis, osoonimise katsetest molekulaarse osooni ja polüaromaatsete süsivesinike reaktsiooni kiiruskonstant $k_{O3,PAH}$ ning O_3/H_2O_2/UV katsetest hüdroksüülradikaalide reaktsiooni kiiruskonstant $k_{OH,PAH}$. Kiiruskonstantide põhjal simuleeriti vastavaid oksüdatsiooniprotsesse. Saadud tulemused näitavad, et koostatud mudelid kirjeldavad oksüdatsiooniprotsesse rahuldavalt, ehkki $k_{OH,PAH}$ väärtuse hindamisel esines mõningaid raskusi. Leiti, et kõigis oksüdatsioonisüsteemides olid määravad molekulaarse osooni reaktsioonid.